DEVELOPMENT OF A NANO-Ni-La-Fe/Al_2O_3 CATALYST TO BE USED FOR SYN-GAS PRODUCTION AND TAR REMOVAL AFTER BIOMASS GASIFICATION

Jianfen Li,[a,b*] Bo Xiao,[b] Rong Yan,[a,c] and Jianjun Liu [a]

The objective of this study was to develop a supported tri-metallic catalyst (nano-Ni-La-Fe/γ-Al_2O_3) for tar removal in biomass steam gasification, to significantly enhance the quality of the produced gas. For this purpose, the supported tri-metallic catalysts were prepared by a deposition-precipitation (DP) method. Different analytical approaches were used to characterize the synthesized catalysts. The results showed that the prepared tri-metallic catalysts had an egg-shell structure with a specific surface area of 214.7 m^2/g. The activity of the catalysts for gas production and tar removal in the process of biomass gasification was also investigated using a bench-scale combined fixed bed reactor. The experiments indicated that the tar yield after adding catalyst was reduced significantly and the efficiency of tar removal reached 99% for the biomass steam gasification at 800°C, while the gas yield after adding catalysts increased markedly and less coke was found over the catalyst. Meanwhile, the compositions of gas products before and after adding catalyst in the process also changed significantly; in particular, the content of hydrogen in catalytic steam gasification was improved by over 10 vol%. Therefore, using the prepared tri-metallic catalyst in biomass gasification can significantly improve the quality of the produced gas and efficiently eliminate the tar generation, preventing coke deposition on the catalyst surfaces, thus demonstrating a long lifetime of the catalyst.

Keywords: Biomass gasification; Catalytic activity; Supported catalyst

*Contact information: a: School of Chemical and Environmental Engineering, Wuhan Polytechnic University, Wuhan, 430023 China; b: School of Environmental Science & Engineering, Huazhong University of Science and Technology, Wuhan,430074, China; c: Institute of Environmental Science and Engineering, Nanyang Technological University, 637723 Singapore; *Corresponding author: lijfen@163.com*

INTRODUCTION

Biomass gasification is one of the promising technologies for converting biomass to bioenergy. One of the major issues in biomass gasification is to deal effectively with the tar formed during the process (Devi et al. 2005). Oil vapor condenses at reduced temperature to form tar, thus causing problems of blocking and fouling in downstream equipment and becoming an environmental concern (Devi et al. 2003). Considerable efforts have therefore been directed towards tar removal from fuel gas. The main approaches applied so far include physical processes such as filters or wet scrubbers, and thermal processes of high-temperature cracking and catalytic cracking. Among these methods, catalytic cracking, which can operate at relatively lower temperatures and generate high tar removal efficiency, is recognized as the most efficient method to

diminish the tar formation in the gas mixture. Catalytic pyrolysis or gasification for tar reduction has been extensively reported in the literature (Corella et al. 2004; Nacken et al. 2007; Sutton et al. 2001). Numerous materials have been tested, but only a few have been found to be active catalysts for tar cracking in biomass gasification or pyrolysis. Ni-based catalysts have been found to be the most popular types and they are very effective for hot gas cleaning (Baker et al. 1987; Furusawa and Tsutsumi 2005; Ma and Baron 2008; Swierczynski et al. 2007; Wang et al. 2005b). Currently, further developments of novel nickel-based catalysts with improved performance are being carried out.

However, most of the commercially available Ni catalysts display a moderate to rapid deactivation due to the build-up of surface carbon and 'sintering' effects (Rapagna et al. 2002). This latter phenomenon occurs at high temperatures; when the nickel is deposited on a support (usually alumina), the metallic particles tend to migrate and form larger aggregates, reducing the dispersion and consequently the catalyst activity. Sintering also favors coke production. As a result, the high specific surface produced with supported systems can become significantly reduced under the reaction conditions employed in biomass gasification. In order to prevent coke deposition on the Ni-catalyst surfaces and 'sintering' effects, some active elements such as lanthanide and iron have been doped in nickel-based catalysts; the strong interactions between the various elements included in a definite chemical structure limit the sintering of the active species as well as carbon build-up. Published studies have established the validity of the Ni-La-Fe tri-metallic catalyst for the reforming reactions of methane (Provendier et al. 1999, 2001; Rapagna et al. 2002). Therefore, the authors have been directing their attention to the supported nano-Ni-La-Fe /γ-Al_2O_3 catalyst and its ternary oxide structures. Nanomaterials have attracted extensive interests for their unique properties such as their catalytic activity (Wang et al. 2005c); in particular, for saving cost, nanometer particles can be loaded on the surface of distinct carriers (such as alumina - Al_2O_3) to prepare the supported catalyst.

This study targeted the development of a novel and low-cost supported nano-Ni-La-Fe catalyst for syn-gas production and tar removal in biomass catalytic gasification. Gamma-alumina was used as a support and urea as a precipitant as well as nickel, lanthanide, and iron salt as metal phase source. The supported nano-Ni-La-Fe/γ-Al_2O_3 catalysts were thus prepared by the deposition-precipitation (DP) method (Burattin et al. 1998; Chang et al. 1998), followed by a series of characterizations using X-ray diffraction (XRD), nitrogen adsorption for surface area (BET), transmission electron microscopy (TEM), and scanning electron microscopy with energy dispersive X-ray analysis (SEM/EDX). Following that, catalytic activity of the prepared supported catalysts was evaluated in a bench-scale combined fixed bed reactor, by comparing biomass steam gasification behaviors with and without catalysts.

EXPERIMENTAL

Catalyst Preparation

The incorporation of the precursor of tri-metallic catalyst into the porous γ-Al_2O_3

support substrates (>99% purity, ~2 mm microsphere) was performed by a deposition–precipitation method, and the preparation conditions of nanometer-sized tri-metallic oxide were selected according to our previous study (Li et al. 2008a,b). The γ-Al_2O_3 supports, which were purchased from the Johnson Matthey Company, were pre-depressurized to a few torr for 1 h to exclude the air from the pores of the support. Urea was selected as a homogeneous precipitation agent to enable a gradual and homogeneous basification of the solution with the increasing temperature to avoid local high pH, which resulted in the subsequent and homogeneous precipitation of nickel precursor in solution; in particular, the urea adsorbed on catalyst would disappear after calcination. To begin, a stoichiometric amount of the reactants, i.e., 0.025mol $Ni(NO_3)_2{\cdot}6H_2O$, 0.01mol $La(NO_3)_3{\cdot}6H_2O$, 0.014mol $Fe(NO_3)_3{\cdot}9H_2O$, and 0.20mol $CO(NH_2)_2$ (urea) were accurately weighed in a beaker and dissolved subsequently into deionized (DI) water. The mixture was stirred with a magnetic stirrer at room temperature until a homogeneous solution was obtained. After that, the homogeneous solution was transferred into a glass vessel containing γ-Al_2O_3 supports (~8g), sealed, and placed in oil bath heating at 115°C for 2.5 h of deposition-precipitation, resulting in precipitation of the precursor (a brown sediment) on γ-Al_2O_3 supports. After the reaction was complete, the mixture was cooled to ambient temperature and then filtered. The brown solid spheres were washed with deionized water to neutral and colorless for removing the possible absorbed ions and chemicals. The brown spheres were then dried in an oven at 90°C for 6 h. Finally, the dried spheres were calcined in a muffle furnace at 550°C for 1 h in air atmosphere. This process would result in the precipitated precursor on support to decompose to tri-metallic oxide. The resulting tri-metallic catalyst products (i.e. nano-Ni-La-Fe/γ-Al_2O_3) were then collected for further analysis.

All the chemicals such as nitrate salts, urea, and alumina used in the preparation of catalyst were analytical grade, and they were used without further purification. Deionized water was used throughout the preparation process.

Catalyst Characterization

The crystalline structures of the supported tri-metallic catalyst product were identified using a Shimadzu XRD-6000 X-ray diffractometer employing Cu Kα radiation (λ = 0.15418 nm). The X-ray tube voltage and current were 40 kV and 30 mA, respectively. The sample was scanned from 10° to 85° (2θ) with a scanning rate of 4˚/min. The average crystallite size of the nano-NiO product was estimated according to the Scherrer equation and further confirmed by the transmission electron microscopy (TEM) results.

A TEM model FEI TECNAIG2, working at 100 kV, was used to understand the grain size and morphology of nanometer particles dispersed on the support surface. For some selected catalyst samples, the elemental distribution of surface and inside the supported catalyst was examined by investigation of a polished radial cross section of the disc, using the scanning electron microscope (SEM) coupled with energy dispersive X-ray spectroscopy (EDX). The analysis was performed on a JSM 5310 LV scanning microscope with an energy dispersive detector.

The metal content in the supported catalysts was measured by X-ray fluorescence (XRF). The equipment used was a Philips PW2400 instrument, made by PANalytical in The Netherlands. The catalyst samples were first ground in alpha-alumina mortars to make sure the particles possessed enough affinity to form self-supported disks for XRF analysis. All samples yielded satisfactory disks after they were pressed at 10 tons of ram load with 2 minutes of bleeding time. The sample disks were then put into the sample cell of a XRF machine that automatically performed the scanning and gave quantitative results as weight percentage (oxide form) of each major element found.

An accelerated Surface Area Porosimetry (ASAP 2010) instrument, which used liquid nitrogen at 77K, was applied to measure the BET surface area of each support and catalyst for estimating its catalytic activity.

Evaluation of Catalytic Activity

The activity of the supported tri-metallic catalyst in biomass catalytic steam gasification was evaluated. The experimental system shown in Fig. 1 consisted essentially of a fixed bed reactor (underlayer fixed bed) combined with another catalytic fixed bed, and with a continuous screw feeding system, a gas cleaning section containing a cyclone solid collector and a quartz wool filter, and a cooling system for the separation of water and condensable organic vapors (tar), as well as various gas measurement devices. The free-fall reactor in the underlayer fixed bed was 200 mm in diameter (ID) × 400 mm in height, and the catalytic fixed reactor was 88 mm in diameter (ID) × 1200 mm in height, constructed of stainless steel with temperature control. Both reactors, which were heated externally, could be separately temperature controlled.

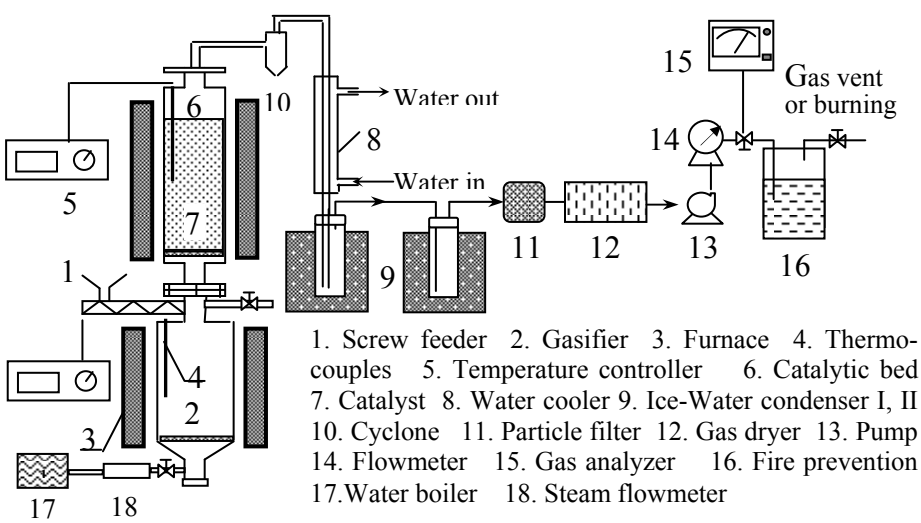

Figure 1. The flow scheme of bench scale reactor

Biomass gasification with or without catalyst was conducted, respectively, under the same process conditions, except for certain exceptions mentioned in the text. When gasification without catalyst was conducted, the under-layer bed was controlled at 800°C while the catalytic bed was empty and its temperature maintained at 200°C for preventing

vapor condensation. However, for catalytic gasification of biomass, the catalytic bed was packed with the supported tri-metallic catalyst (1 kg) or nano-NiO/γ-Al_2O_3 (as a reference). The underlayer fixed bed temperature was always maintained at 800°C, and the catalytic bed temperature was maintained respectively at 750°C, 800°C and 850°C.

Sawdust (in particle size 0.15-2 mm) was used as the raw material. It was stocked in a hopper and fed into the reactor via a screw feeder at a rate of 1 kg/h, when the desired temperature was reached. Then, the steam in the steam generator was provided via a steam flowmeter at a velocity of 0.6kg/h. The generated vapors in the hot reactor with fine particles were drawn out by the vacuum pump, which passed through the cyclone and quartz wool filter for the fine particles removal. The condensable component was quenched when gas passed through the water-cooling tube and two ice-water condensers in series. After every experiment, the liquid (including water and tar) in the cooling tube and condensers was collected and further separated into aqueous and oil fractions using the standard ASTM D244 and IP 291.1 methods. The oil fraction was weighed and recorded as the tar yield. The total volume of the generated gas could be measured by a gas flowmeter, and the total gas yield (Nm^3/kg) could thus be calculated based on the consumed biomass in a specific time period at a constant feeding rate. Those uncondensable gases were pre-cleaned through a glass wool filter and dried by silica gels prior to analysis. The gas products were analyzed using a dual Channels Micro-Gas Chromatograph (Micro-GC, Varian, CP-4900) with a thermal conductive detector (TCD). The detailed measuring procedure can be found in our previous publication (Yang et al. 2006). Each trial was maintained for a period of 30 min, and several repeat runs were carried out under identical conditions to ensure the repeatability of the process.

In addition, it is recognized that Ni metal serves as the active ingredient in the Ni-based catalysts; thus the developed catalysts and the reference catalyst Nano-NiO/Al_2O_3 should be first reduced by hydrogen before the experiment. On the other hand, some earlier research (Martinez et al. 2004; Zhang et al. 2004) indicated that the commercial and doping Ni-based catalyst without reduction could be used in biomass catalytic gasification, as the catalyst could be reduced and activated by the resulting gas (including H_2 and CO) in the initial gasification period. With the focus of this study on the preparation and evaluation of a supported tri-metallic catalyst, the performance of the developed catalyst was evaluated in comparison with nano-NiO/Al_2O_3 catalyst in the same conditions, where the pre-reduction of catalysts was ignored for a purpose of simplification.

RESULTS AND DISCUSSION

Analysis and Characterization of the Catalyst

Appearance and XRF analysis

The supported tri-metallic catalysts prepared by the DP method were found to be spherical in shape and brown in color. The content of metal oxide in the supported catalysts was measured using XRF. The content of NiO, Fe_2O_3, and La_2O_3 in catalysts prepared at 550°C was 8.6%, 7.4%, and 5.9%, respectively. For the purpose of

comparison, the impregnation method for preparing catalyst was also tested, where γ-Al_2O_3 was impregnated in a solution of the tri-metallic nitrate salts followed by calcinations under the same conditions. The results showed that the tri-metallic oxide total loading of catalysts prepared by impregnation were all less than 5%. The DP of metal precursors on supports was thus recognized to yield higher metal loading over the impregnation method. Similar findings were reported by Chang et al. (1998) in the preparation of rice husk ash supported nickel catalyst.

XRD analysis

X-ray diffractions of catalyst products were carried out to identify the phases present in the supported tri-metallic catalyst samples, and the results are presented in Fig. 2. The XRD profiles of catalyst samples obtained at calcination temperature 550 °C showed that NiO, La_2O_3, α-Fe_2O_3, and γ-Al_2O_3 were the main phases. Owing to the fact that γ-Al_2O_3 was the main component of support, thus NiO, α-Fe_2O_3, and La_2O_3 nanoparticles were the active components of the catalyst. According to Scherrer's equation: D=0.89λ/βcosθ, where D represents the average particle size, β stands for the full-width at half-height of the peaks, λ is the wavelength of X-ray, and θ is the diffraction angle of the peak. The mean particle size of the nanocrystalline tri-metallic oxide on catalyst samples' surface was thus calculated at about 32 nm. This was confirmed by its TEM images.

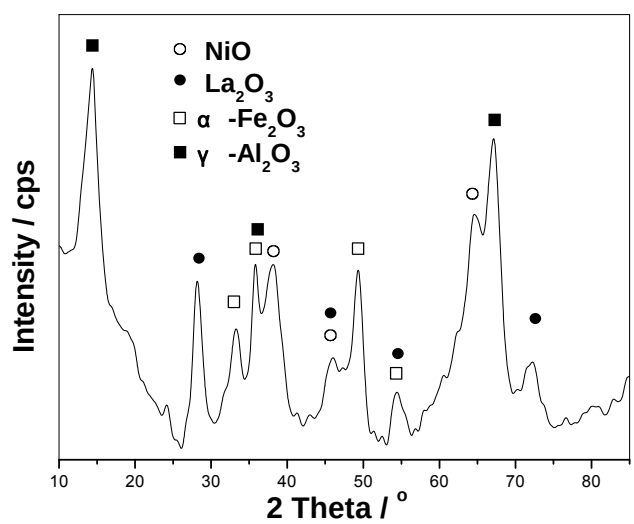

Figure 2. XRD pattern of the supported tri-metallic catalyst samples

TEM and SEM/EDX analysis

TEM and SEM/EDX analyses of the supported catalysts were performed, and only representative images are presented here. The TEM micrograph of tri-metallic oxide nano-particles on catalyst surface is shown in Fig. 3. It can be seen that the nano-particles on catalyst surface were spherical in shape. The size of nanoparticles was between 28 and 35 nm, which coincided with the XRD results of catalysts.

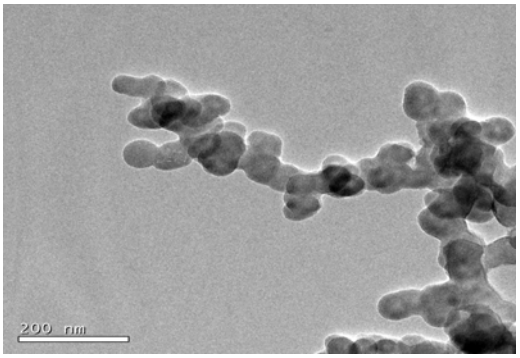

Figure 3. TEM micrograph of nano-particles on the tri-metallic catalyst surface

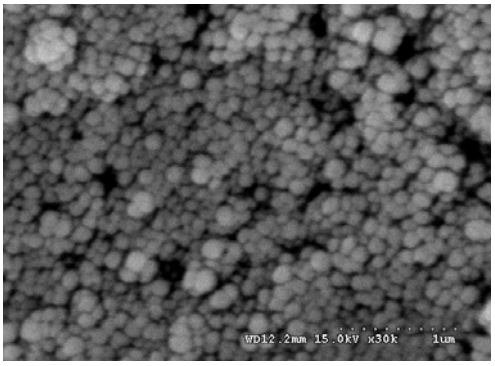

Figure 4. SEM image of the supported tri-metallic catalyst surface

The SEM appearance image of the catalyst surface is shown in Fig. 4. The surface of the catalyst was scraggy, and nanoparticles displayed a fairly uniform spatial distribution on the surface. These are all positive factors for the catalytic application (Ma and Baron 2008; Nacken et al. 2007).

To further confirm the structure and elemental distribution on the surface and inside catalyst, the catalyst samples were cut, and the corresponding elemental distributions on the surface of cross-section and inside catalyst were obtained by EDX with a square analysis window of about 200nm. The EDX analysis showed that the inside of the catalyst consisted exclusively of the elements Al and O, with a content respectively of 46.62% and 53.38%. But at the surface of the catalyst five elements (Ni, Fe, La, Al and O) were mainly observed, with their contents respectively at 22.05%, 20.13%, 18.22%, 1.52%, and 38.08%. This further confirmed that the prepared catalyst by DP method had a typical coated eggshell-type structure, where the tri-metallic oxide nanoparticles mainly coated the surface of the γ-Al_2O_3 spheres. The core parts were γ-Al_2O_3, and the shell layers were enriched in tri-metallic oxide nanoparticles. In the meantime, the above observations also indicated that no Ni, La, or Fe was found inside of the catalyst, and the main composition of the catalyst surface was tri-metallic oxide with few Al-bearing compounds, which were attributed to the interaction of tri-metallic oxide nanoparticles with the alumina support. With respect to the heterogeneous catalysts, the active sites of the catalyst are the available surface and not the inside; thus the coated structure of the supported catalyst prepared by DP method in this study can save costs significantly, resulting from the much reduced of usage of tri-metallic salt in the preparation process.

BET analysis

The surface properties of the γ-Al_2O_3 support and the supported catalysts were evaluated from the nitrogen adsorption-desorption isotherms using the ASAP 2010 instrument, and the results are summarized in Table 1. The supported tri-metallic catalysts exhibited nitrogen isotherms with the same shape as that of the support. The

catalysts had a relatively high specific surface area, but a slight reduction of the BET surface area and pore volume compared with that of γ-Al_2O_3 support. This decrease could be attributed to not only to the presence of tri-metallic oxide particles partially blocking the porous network of support, but also to the increase in the density of the materials after the incorporation of a tri-metallic oxide loading as high as above 21 wt-%.

Table 1 showed that the BET specific and external surface areas of the supported tri-metallic catalysts in current study were much higher than that of the commercial nickel based catalyst, which were reported to be less than 90 m^2/g of BET surface area and 85 m^2/g of external surface area (Zhang et al. 2004). This was most likely attributable to the smaller size of tri-metallic oxide nanoparticles on the surface of the supported catalysts. The BET specific and external surface areas of the NiO/γ-Al_2O_3 catalyst are also listed in Table 1, which shows that they were lower than that of tri-metallic catalysts, too. The preparation method and performance of the NiO/γ-Al_2O_3 catalyst can be found in our previous publication (Li et al. 2008b). The higher BET specific and external surface areas of the supported tri-metallic catalysts indicated its high possibility of application as an efficient catalytic material.

Table 1. Surface Properties of Catalysts Measured by N_2 Physisorption

Catalyst Sample and Support	BET surface area (m^2/g)	Micro pore area (m^2/g)	External surface area (m^2/g)	Total pore volume (cm^3/g)	Average pore diameter (nm)
Support, γ-Al_2O_3 (1.5mm)	256.8	24.4	232.4	0.39	6.8
The Supported Catalyst	214.7	19.4	195.3	0.41	8.2
The NiO/γ-Al_2O_3 Catalyst	124.6	10.0	114.7	0.37	12.3

Evaluation of the Catalyst for Biomass Steam Gasification

Comparison of product yield before and after adding catalyst

Table 2 shows the product yields from steam gasification and catalytic gasification of sawdust. It can be seen from Table 2 that the gas yield (Nm^3/kg biomass, wet basis) at 800°C steam gasification in the absence of catalyst was 1.22 Nm^3/kg; however, when the vapors were passed through the catalytic bed with the supported tri-metallic catalyst at 700°C, there was a marked increase in gas yield. In the meantime, the yield of gases increased from 1.88 to 2.40 Nm^3/kg as the catalytic bed temperature increased from 750 to 850°C. The significant increase in gaseous yield was attributed to be predominantly through secondary cracking of the vapors on the catalyst in the catalytic bed reactor. A similar finding on other catalysts for biomass steam gasification was also reported by Lv et al. (2004). For purpose of comparison, the supported nano-NiO/γ-Al_2O_3 catalysts (NiO content of 12 wt-%) were loaded in the catalytic reactor for catalytic steam gasification of sawdust under the same conditions at 800°C. The results showed that gas yield at 800°C gasification in the presence of nano-NiO/γ-Al_2O_3 catalysts was 2.04 Nm^3/kg, which was lower than that of the tri-metallic catalyst under the same conditions. Therefore, the supported tri-metallic catalyst was more effective

over nano-NiO/γ-Al_2O_3 catalysts in enhancing the gas yield of sawdust steam gasification.

Table 2. Product Yields from Steam Gasification and Catalytic Gasification of Sawdust (g/Nm^3 for tar, and Nm^3/kg biomass for gas, wet basis)

Conditions	Gas Nm^3/kg	Tar g/Nm^3
Sawdust steam gasification without catalyst at 800 °C	1.22	38.60
Catalytic gasification with NiO/γ-Al_2O_3 catalyst at 800 °C	2.04	0.42
Catalytic gasification with tri-metallic catalyst		
750 °C	1.88	0.48
800 °C	2.16	0.24
850 °C	2.40	0.08

For the steam gasification of sawdust in the absence of catalysts, the derived liquid was yellow in colour, whereas for all the liquid products derived from the catalytic steam gasification of sawdust at 800°C, scarcely any visible tar was observed in the line after the catalytic reactor or in the condensers for tar collecting. The collected condensed portions were further separated into aqueous and oil fractions using the standard ASTM D244 and IP 291.1 methods, to determine the total tar yield. In the absence of catalyst, the tar yield from the steam gasification of sawdust was 38.60 g/Nm^3, as shown in Table 2. After adding the tri-metallic catalyst it fell to only 0.48 g/Nm^3 at 750°C, and was reduced further to 0.24 g/Nm^3 at 800°C, and 0.08 g/Nm^3 as the temperature of catalytic bed was increased to 850°C. For a comparison, the nano-NiO/γ-Al_2O_3 catalyst was also used in steam gasification of sawdust under exactly the same conditions at 800°C. In Table 2, it can be seen that the catalytic efficiency of the tri-metallic catalyst for tar removal was slightly better than that of the nano-NiO/γ-Al_2O_3 catalyst. This indicated that the developed tri-metallic catalyst could have a high performance for valuable gas production and tar removal in catalyzing biomass gasification, even at a relatively low temperature.

Various commercial nickel-based catalysts were reported in previous literature for tar removal and improvement of the produced gas quality. For instance, Corella et al. (1999) tested seven commercial Ni-based catalysts (NiO content of 12-25 wt%), which all were shown to be very active, with about 95% tar removal easily obtained at 800-850°C. However, their results were all based on crushed particles of the catalyst. For commercial application the effectiveness factors of 1-10% (only) might have to be applied. In this study, the tar removal efficiency exceeded 99% at 800°C, indicating that the prepared tri-metallic catalyst was ideal for tar removal in biomass gasification, with a high efficiency in comparison with the commercial and other nickel-based catalysts.

Comparison of gas composition before and after adding catalyst

Table 3 shows the percentage in volume of product gas components for the steam gasification at 800°C and catalytic steam gasification at respectively 750, 800, and 850°C. The results showed that the main gas products were H_2, CO, CO_2, and CH_4, with less C_2 hydrocarbons (C_2H_4 and C_2H_6). Comparing gas composition from the steam gasification of sawdust with tri-metallic catalyst and without catalyst in Table 3, it could be seen that the content of hydrogen in catalytic steam gasification was improved over 10 vol %; CO and CO_2 content had an obvious decrease; nearly half of CH_4 was converted; and C_2 content was lowered to below 1 vol-%. From these changes of gas composition, it could be concluded that several important reactions, such as the water shift reaction (Eqs. 1 and 2) and hydrocarbon reforming reaction (Eqs. 3 and 4), occurred. All those reactions are favorable for hydrogen generation, thus the content of H_2 in gas increased significantly, while the hydrocarbon was consumed, resulting in the sharp reduction of CH_4 and C_2 contents. CO and CO_2 were produced through reactions 1-4, but in the meantime they were consumed via other reactions 1 and 3; thus their final contents decreased obviously due to the overall effect of these reactions and the marked increase of H_2 content in gas.

$$CO + H_2O = CO_2 + H_2 \quad (1)$$
$$C + H_2O = CO + H_2 \quad (2)$$
$$C_nH_m + nCO_2 = 2nCO + (m/2)H_2 \quad (3)$$
$$C_nH_m + nH_2O = nCO + (n+m/2)H_2 \quad (4)$$

Table 3. Gas Composition from the Steam Gasification of Sawdust with and without Catalyst (vol-%)

Conditions	H_2	CO	CO_2	CH_4	C_2H_4	C_2H_6
Sawdust steam gasification without catalyst at 800 °C	38.6	25.1	27.1	7.4	1.0	0.8
Catalytic gasification with NiO/γ-Al_2O_3 catalyst at 800 °C	54.4	20.4	20.5	4.2	0.3	0.2
Catalytic gasification with tri-metallic catalyst						
750 °C	51.6	22.4	20.3	4.9	0.5	0.3
800 °C	53.8	20.6	20.8	4.3	0.3	0.2
850 °C	56.6	18.1	22.6	2.5	0.1	0.1

Table 3 also shows the effect of temperature in the catalytic reactor on gas composition. As the temperature of the catalytic reactor increased from 750 to 850°C, the content of H_2 and CO_2 increased, while that of the other gases such as CO, CH_4, and C_2 decreased. This could be attributed to the promotion of a higher temperature on the endothermic steam reforming reactions and water shift reaction. All those reactions 1-4 were strengthened with increasing temperature, which resulted in an increase of H_2

content and a decrease of CH_4 and C_2 content. As to the variation trends of gas composition for CO and CO_2, which were mainly determined by reaction 1 due to the quick reaction velocity and the high and stable steam concentration, CO was produced through reactions 2 and 3, but simultaneously consumed mainly via the reaction 1 to generate CO_2, which led to a decline of CO content and enhancement of CO_2 content.

Caballero et al. (1997) and Lv et al. (2004) have performed studies on catalytic biomass steam gasification. Comparing this study and the aforementioned works, it could be found that as to the variation of gas composition for H_2, CH_4, and C_2 after the catalytic reactor, the trends were the same. As to the variation of gas composition for CO and CO_2, the trends had a little difference, which had also presented itself to different researchers. In the study of Caballero et al., CO content increased while CO_2 content decreased after the catalytic reactor; opposite trends were reported in the study of Lv et al. This difference possibly came from the different reactor, operating conditions, and gasifying agents used.

For easy comparison, the gas product percentages with presence of nano-NiO/γ-Al_2O_3 catalyst at 800°C are also listed in Table 3. Compared with the supported nano-NiO/γ-Al_2O_3 catalyst under the same conditions, the addition of lanthanum and iron to the nano-NiO/γ-Al_2O_3 catalyst resulted in a minor increase in CO, CO_2, CH_4, C_2 and total gas yields, while the H_2 yield remained almost unchanged. This demonstrates that with nano-Ni-La-Fe/γ-Al_2O_3 catalysts, there was higher transformation of the carbon contained in the biomass to valuable gases and, consequently, less coke was formed over the catalyst.

For tar removal and improvement of the produced gas quality during biomass gasification process, the function of Fe_2O_3 and La_2O_3 in the nickel-based catalysts has been also studied by Wang et al. (2005a) and Martinez et al. (2004), respectively. Wang et al. investigated cracking of biomass tar over Ni/dolomite catalyst, including various concentrations of Fe_2O_3, which indicated that the catalyst was highly effective for the removal of biomass tar and adjustment of the gas composition to syngas quality, and the excellent activity of catalyst may be attributed to the high Fe_2O_3 content in the catalyst. Martinez et al. studied the influence of lanthanum to Ni–Al catalysts for steam gasification of biomass, which demonstrated that the addition of 4-12 wt% La to Ni–Al catalyst facilitated the diminution of coke deposition and a higher gas yield, since the acidity of the support decreases, owing to the La_2O_3 basicity. These results were in agreement with that of the current work, in which 7.4 % Fe_2O_3 and 5.9% La_2O_3 were added in current nickel-based catalysts for reducing the cost of catalyst because of the high price of La_2O_3.

The aforementioned results indicated that the prepared tri-metallic catalyst enhanced markedly the cracking of tar in vapor and of hydrocarbons such as CH_4 and C_nH_m in gaseous products to convert them to valuable H_2 and CO, owing to the catalysis-assisted decomposition of tar and possibly the lengthening of vapor residence time inside the catalytic bed. In particular, the content of H_2 in gas components was enhanced significantly, while that of CH_4 decreased. Therefore, the tri-metallic catalyst exhibited excellent catalytic activity for tar removal and the valuable H_2 generation. It was evidenced that the prepared tri-metallic catalyst could improve significantly the quality of

the produced gas and remove efficiently tar presented in the vapour phase of biomass steam gasification.

Lifetime test for the supported tri-metallic catalyst

Once deactivation of nickel-based catalysts is proven in a biomass gasification process, it is usually attributed to three main causes: sulfur poisoning, coke deposition (mainly from tar), and sintering. Usually the sulfur content is very low in biomass and in the thus-produced gas (Lv et al. 2004). Therefore, the main purpose of this test was to indicate performance of the supported tri-metallic catalysts preventing coke deactivation and sintering effects. This experiment was respectively performed to load two different catalysts for the supported tri-metallic catalysts and nano-NiO/γ-Al_2O_3 catalyst in the catalytic reactor at 800°C, while the other conditions in the gasifier were kept constant besides the catalyst. Each test lasted as long as 10 hours. The test results are shown in Fig. 5, which indicates nearly no deactivation for the supported tri-metallic catalysts and a little deactivation for nano-NiO/γ-Al_2O_3 catalyst in biomass steam gasification process. Meanwhile, comparing the XRD patterns of two catalysts before and after use, the results revealed nearly no difference for the XRD patterns of the supported tri-metallic catalysts before and after use, and no generation of new phases. However, two new phases such as carbon and $NiAl_2O_4$ (spinel structure) appeared in the XRD patterns of nano-NiO/γ-Al_2O_3 catalyst after use, and all the diffraction peaks were markedly sharpening with high intensities; these results suggested that coke deposited on the used nano-NiO/γ-Al_2O_3 catalyst and the Ni-catalyst was sintered to lead to the deactivation of the catalyst.

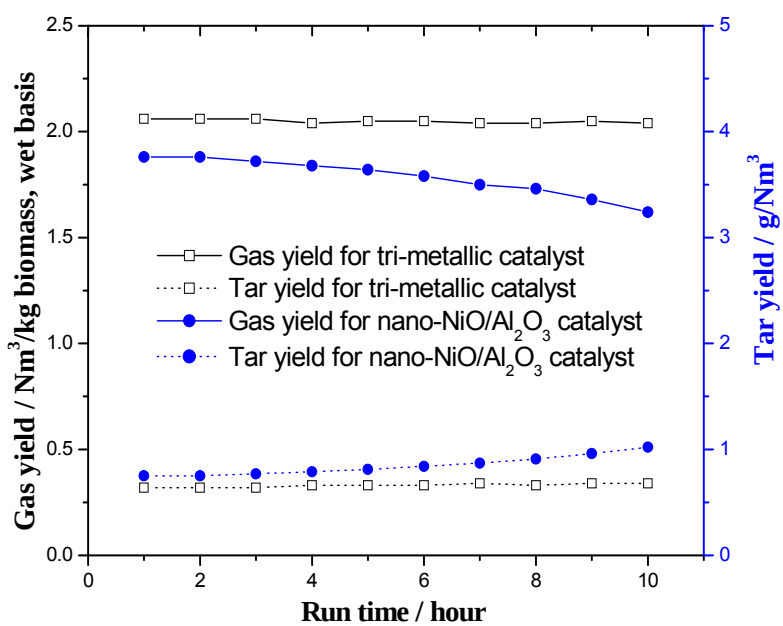

Figure 5. Lifetime test for the supported catalysts

Thermal analysis of two catalysts for the tri-metallic catalyst and nano-NiO/γ-Al_2O_3 catalyst after use was also carried out in a thermogravimetric analyzer (NETZSCH STA 409C, Germany) to verify the coke deposition on the used catalyst surface. The used

catalysts were heated at a rate of 10°C/ min in airflow from the room temperature up to 850°C. The results showed that there was no obvious weight loss and exothermic peak in TG and DSC curves of the tri-metallic catalyst. However, for the used nano-NiO/γ-Al_2O_3 catalyst, two distinct intervals of weight loss were observed in the TG curve, accompanied by two obvious exothermic peaks located between 450 and 580 °C in the DSC curve, which was attributed to coke deposition on the used catalyst surface. Therefore, these experiments demonstrated that the supported tri-metallic catalyst has a long lifetime to prevent coke deactivation and sintering, which can be attributed to the lanthanide and iron doped in the tri-metallic catalyst, effectively limiting the sintering of the active species in catalyst, as well as limiting coke deposition.

CONCLUSIONS

1. The supported tri-metallic catalyst was prepared by a deposition-precipitation method, and its physical/chemical properties were fully characterized by different analytical approaches. The results showed that the prepared tri-metallic catalysts had a coated structure with over 21 wt-% tri-metallic oxides loading in the catalysts. The tri-metallic oxide nanoparticles as the active components of catalyst were located at the catalyst surface with a size range of 28 to 35 nm. The prepared tri-metallic catalyst was mainly comprised of NiO, La_2O_3, α-Fe_2O_3, and γ-Al_2O_3 phases, and it had a higher BET surface area of 214.7m^2/g, which was greater than that of the commercial nickel based catalyst and NiO/γ-Al_2O_3 catalyst.
2. The activity of the prepared tri-metallic catalyst in biomass steam gasification was evaluated. The performance of the catalyst was recognized by comparing the cases with and without catalyst, in terms of the tar and gas yield and gas product composition. The tar yield after adding catalyst was reduced significantly, with the tar removal efficiency reaching 99% for catalytic gasification at 800°C, while the gas yield markedly increased with adding catalyst. The percentages of C_2 and CH_4 in the product gas after catalysis were obviously reduced, while that of the valuable H_2 increased markedly to over 10 vol-% due to catalysis.
3. Compared with the nano-NiO/γ-Al_2O_3 catalyst, the addition of lanthanum and iron to the NiO/γ-Al_2O_3 catalyst resulted in an increase in CO, CO_2, CH_4, C_2, and total gas yields for biomass steam gasification, while the H_2 yield remained almost unchanged. This demonstrates that with the tri-metallic catalysts, a higher transformation of the carbon contained in the biomass to valuable gases takes place and, consequently, less coke is formed over the catalyst. Therefore, using the prepared tri-metallic catalyst in biomass gasification could improve significantly the quality of the produced gas and remove efficiently tar presented in the vapour of biomass gasification, especially preventing coke deposition on the catalyst surfaces and sintering effects to achieve a long lifetime.

ACKNOWLEDGMENTS

The authors are grateful for the financial support of the National Natural Science Foundation of China (Grant. No. 20876066) and Natural Science Foundation of Hubei Province (Project No. 2008CDA033).

This article was presented at the First International Conference on Biomass Energy Technologies (ICBT 2008), which was held at the Baiyun International Convention Center, Guangzhou, China, and hosted by Chinese Renewable Energy Society and its affiliate Chinese Bioenergy Association during December 3-5, 2008. Sponsors were the National Development and Reform Commission (NDRC), the Ministry of Science and Technology of the People's Republic of China (MOST), and the Ministry of Agriculture of the People's Republic of China (MOA) and Chinese Academy of Sciences (CAS). Selected articles from the conference were submitted to *BioResources* and subjected to the standard peer-review process.

REFERENCES CITED

Baker, E. G., Mudge, L. K., and Brown, M. D. (1987). "Steam gasification of biomass with nickel secondary catalysts," *Ind. Eng. Chem. Res.* 26(7), 1335-1339.

Burattin, P., Che, M., and Louis, C. (1998). "Molecular approach to the mechanism of deposition - Precipitation of the Ni(II) phase on silica," *J. Phys. Chem. B*, 102(15), 2722-2732.

Caballero, M. A., Aznar, M. P., Gil, J., Martin, J. A., Frances, E., and Corella, J. (1997). "Commercial steam reforming catalysts to improve biomass gasification with steam-oxygen mixtures. 1. Hot gas upgrading by the catalytic reactor," *Ind. Eng. Chem. Res.* 36(12), 5227-5239.

Chang, F. W., Hsiao, T. J., and Shih, J. D. (1998). "Hydrogenation of CO_2 over a rice husk ash supported nickel catalyst prepared by deposition-precipitation," *Ind. Eng. Chem. Res.* 37(10), 3838-3845.

Corella, J., Orio, A., and Toledo, J. M. (1999). "Biomass gasification with air in a fluidized bed: exhaustive tar elimination with commercial steam reforming catalysts," *Energy Fuels* 13(3), 702-709.

Corella, J., Toledo, J. M., and Padilla, R. (2004). "Catalytic hot gas cleaning with monoliths in biomass gasification in fluidized beds. 1. Their effectiveness for tar elimination," *Ind. Eng. Chem. Res.* 43(10), 2433-2445.

Devi, L., Ptasinski, K. J., and Janssen, F. J. G. (2003). "A review of the primary measures for tar elimination in biomass gasification processes," *Biomass and Bioenergy* 24(2), 125-140.

Devi, L., Ptasinski, K. J., and Janssen, F. J. J. G. (2005). "Pretreated olivine as tar removal catalyst for biomass gasifiers: investigation using naphthalene as model biomass tar," *Fuel Processing Technology* 86(6), 707-730.

Furusawa, T., and Tsutsumi, A. (2005). "Comparison of Co/MgO and Ni/MgO catalysts for the steam reforming of naphthalene as a model compound of tar derived from biomass gasification," *Applied Catalysis A: General* 278(2), 207-212.

Li, J., Yan, R., Xiao, B., Liang, D. T., and Lee, D. H. (2008a). "Preparation of nano-NiO particles and evaluation of their catalytic activity in pyrolyzing biomass components," *Energy Fuels* 22(1), 16-23.

Li, J., Yan, R., Xiao, B., Liang, T. D., and Du, L. (2008b). "Development of nano-NiO/Al_2O_3 catalyst to be used for tar removal in biomass gasification," *Environmental Science & Technology* 42 (16), 6224-6229.

Lv, P., Chang, J., Wang, T., Fu, Y., and Chen, Y. (2004). "Hydrogen-rich gas production from biomass catalytic gasification,." *Energy & Fuels* 18, 228-233.

Ma, L., and Baron, G. V. (2008). "Mixed zirconia–alumina supports for Ni/MgO based catalytic filters for biomass fuel gas cleaning," *Powder Technology* 180, 21-29.

Martinez, R., Romero, E., Garcia, L., and Bilbao, R. (2004). "The effect of lanthanum on Ni-Al catalyst for catalytic steam gasification of pine sawdust," *Fuel Processing Technology* 85(2-3), 201-214.

Nacken, M., Ma, L., Engelen, K., Heidenreich, S., and Baron, G. V. (2007). "Development of a tar reforming catalyst for integration in a ceramic filter element and use in hot gas cleaning," *Ind. Eng. Chem. Res.* 46(7), 1945-1951.

Provendier, H., Petit, C., Estournes, C., Libs, S., and Kiennemann, A. (1999). "Stabilisation of active nickel catalysts in partial oxidation of methane to synthesis gas by iron addition," *Applied Catalysis A: General* 180(1-2), 163-173.

Provendier, H., Petit, C., and Kiennemann, A. (2001). "Steam reforming of methane on LaNixFe1-xO3 (0<=x<=1) perovskites. Reactivity and characterisation after test," *Comptes Rendus de l'Academie des Sciences - Series IIC - Chemistry* 4(1), 57-66.

Rapagna, S., Provendier, H., Petit, C., Kiennemann, A., and Foscolo, P. U. (2002). "Development of catalysts suitable for hydrogen or syn-gas production from biomass gasification," *Biomass and Bioenergy* 22(5), 377-388.

Sutton, D., Kelleher, B., and Ross, J. R. H. (2001). "Review of literature on catalysts for biomass gasification," *Fuel Processing Technology* 73(3), 155-173.

Swierczynski, D., Libs, S., Courson, C., and Kiennemann, A. (2007). "Steam reforming of tar from a biomass gasification process over Ni/olivine catalyst using toluene as a model compound," *Applied Catalysis B: Environmental* 74(3-4), 211-222.

Wang, T., Chang, J., and Lv, P. (2005a). "Novel catalyst for cracking of biomass tar," *Energy & Fuels* 19(1), 22-27.

Wang, T. J., Chang, J., Wu, C. Z., Fu, Y., and Chen, Y. (2005b). "The steam reforming of naphthalene over a nickel-dolomite cracking catalyst," *Biomass and Bioenergy* 28(5), 508-514.

Wang, Y., Zhu, J., Yang, X., Lu, L., and Wang, X. (2005c). "Preparation of NiO nanoparticles and their catalytic activity in the thermal decomposition of ammonium perchlorate," *Thermochimica Acta* 437(1-2), 106-109.

Yang, H. P., Yan, R., Chen, H. P., Lee, D. H., Liang, D. T., and Zheng, C. G. (2006). "Pyrolysis of palm oil wastes for enhanced production of hydrogen rich gases," *Fuel Processing Technology* 87(10), 935-942.

Zhang, R., Brown, R. C., Suby, A., and Cummer, K. (2004). "Catalytic destruction of tar in biomass derived producer gas," *Energy Conversion and Management* 45(7-8), 995-1014.

Date submitted: April 1, 2009; Peer review completed: April 21, 2009; Revised version accepted: Sept. 24, 2009; Published: Sept. 27, 2009.